Nonequilibrium optical phonon generation by steady-state electron transport in quantum-cascade lasers

Vincenzo Spagnolo[a] and Gaetano Scamarcio[b]
Dipartimento Interateneo di Fisica, INFM, Università e Politecnico di Bari, via Amendola 173, 70126 Bari, Italy

Mariano Troccoli, Federico Capasso, Claire Gmachl, A. Michael Sergent, Albert L. Hutchinson, Deborah L. Sivco, and Alfred Y. Cho
Bell Laboratories, Lucent Technologies, 600 Mountain Avenue, Murray Hill, New Jersey 07974

(Received 18 February 2002; accepted for publication 27 March 2002)

Observation of the nonequilibrium optical phonons population associated with electron transport in quantum-cascade lasers is reported. The phonon occupation number was measured in the range 75–280 K by using a combination of microprobe photoluminescence and Stokes/anti-Stokes Raman spectroscopy. The excess phonon population is observed to decrease as the lattice temperature increases. From the nonequilibrium phonon population, we extracted interface phonon lifetimes of 5 ps at 75 K and 2 ps at 280 K. © *2002 American Institute of Physics.* [DOI: 10.1063/1.1481186]

The emission of optical phonon is the dominant process controlling energy relaxation of carriers in semiconductors.[1] The typical value for the electron–optical phonon scattering rate is $(2\ \mathrm{ps})^{-1}$, while the lifetime of optical phonons is in the range 3–9 ps.[1,2] Thus, if the excited carrier densities are large, optical phonon emission can be rapid enough to raise the occupation number N of the strongly interacting modes above the thermal equilibrium value N_0, thereby creating a so-called hot phonon population $N=N_0+N'$.

The presence of a hot phonon population strongly affects all major electronic transport and optical characteristics and leads to the enhancement of the phonon absorption rates, thereby reducing the net energy and momentum loss rates of carriers.[3,4] Nonequilibrium optical–phonon populations have been created by energy relaxation of photoexcited carriers.[5–7] Electrical methods to generate nonequilibrium populations of selected phonons have been proposed.[8,9] However, at present only the amplification of acoustic modes with frequency <10 GHz has been demonstrated, exploiting the effect of electron drift velocities higher than the sound velocity.[10]

Electrically driven semiconductor sources of high-frequency phonons are highly desirable. Their availability would allow to directly probe electron–phonon and phonon–phonon scattering phenomena, electronic defects, and interface states even in buried quantum heterostructures[11] and for the generation of high-frequency phonon beams used in phonon optics and phonon imaging studies.

In this letter we report the observation of a nonequilibrium optical phonon population generated by electron transport in quantum cascade (QC) lasers operated in dc mode below laser threshold, using a combination of microprobe Stokes/anti-Stokes (S/AS) Raman and photoluminescence (PL) spectroscopy.

QC lasers exploit the electron–phonon interaction to achieve population inversion between different subbands in the conduction band.[12] This process, schematically illustrated in Fig. 1 for the active region of a QC laser emitting at $\lambda \sim 8\ \mu$m (155 meV),[13] takes to the generation of an average number of 4–6 optical phonons per stage for each electron injected into the upper laser level [$n=3$ in Fig. 1(b)]. This effect is amplified by the typically large (10–30) number of active stages. The large optical phonon generation rates achieved in QC structures have a strong influence on the laser operation,[14,15] but could be exploited to use this kind of laser as a source of optical phonons.

We investigated a laser structure including a 0.53 μm thick active region composed of 12 periods of a $Al_{0.48}In_{0.52}As/Ga_{0.47}In_{0.53}As$ heterostructure. The layer sequence is listed in the caption of Fig. 1(a). The waveguide core consists of an active region sandwiched between two 0.5 μm thick $Ga_{0.47}In_{0.53}As$ layers. The complete structure also includes a top cladding layer composed of a 2.5 μm thick $Al_{0.48}In_{0.52}As$ layer and a 0.5 μm thick $Ga_{0.47}In_{0.53}As$ layer. The InP substrate acts as the lower cladding. The mid-infrared optical performance and electrical characteristics have been reported elsewhere (sample D2405 of Ref. 13).

In QC lasers, the strongest electron–phonon interaction is associated with in-plane propagating interface (IF) phonons.[16–18] The IF phonons of the GaInAs/AlInAs active region can be grouped in four branches: IF^{I}_{InAs} (28–29 meV) and IF_{GaAs} (30–32 meV) phonons associated with GaInAs; IF^{II}_{InAs} (27.5–29 meV) and IF_{AlAs} (42.5–45.5 meV) phonons associated with AlInAs. The IF_{GaAs} modes are suitable probes of the phonon population in the active region. The two $IF^{I,II}_{InAs}$ branches instead cannot be spectrally resolved because of the quite large linewidth ($\sim 15\ \mathrm{cm}^{-1}$) of the Raman bands due to alloy broadening. The Bose population factor of the IF_{AlAs} modes is 1 order of magnitude smaller than that of $IF^{I,II}_{InAs}$ and IF_{GaAs} modes at temperatures below 150 K, giving hardly detectable anti-Stokes signals. In the case of bulk AlInAs and InP cladding layers the phonon population can be measured by studying the transverse optical (TO) phonon modes.

[a] Author to whom correspondence should be addressed; electronic mail: spagnolo@fisica.uniba.it
[b] Electronic mail: scamarcio@fisica.uniba.it

 © 2002 American Institute of Physics
Downloaded 22 May 2008 to 128.103.60.225. Redistribution subject to AIP license or copyright; see http://apl.aip.org/apl/copyright.jsp

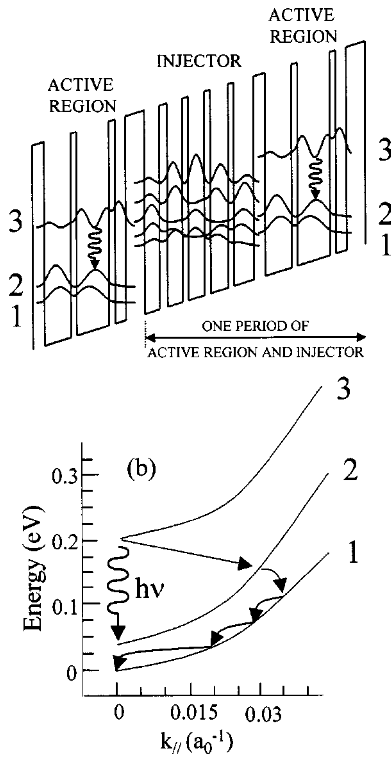

FIG. 1. (a) Calculated conduction-band structure of the QC device under an applied electric field of 40 kV/cm. The AlInAs/GaInAs layer thickness sequence in one period, starting from the injector AlInAs barrier (rightmost layer), is 3.8/2.1/1.2/6.5/1.2/5.3/2.3/4.0/1.1/3.6/1.2/3.2/1.2/3.0/1.6/3.0, expressed in nm. The underlined layers are Si doped to $n=2\times10^{17}$ cm^{-3}. The moduli squared of the wave functions involved in the laser transition (labeled 1, 2, and 3) and of the injector wave-functions manifold, are also shown. The laser transition is indicated by the wavy arrows. (b) Energy dispersion of the 1–3 subbands, as a function of the wave number parallel to the layers ($k_{\parallel}$), expressed in units of reciprocal Bohr radius a_0^{-1}. One of the many possible electron relaxation routes by emission of optical phonons to the bottom of the lower subband is shown.

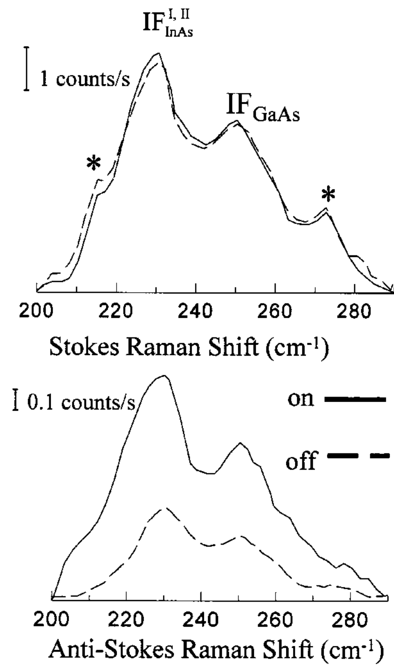

FIG. 2. Stokes and anti-Stokes Raman spectra measured from the active region of a substrate-side mounted QC laser with the device off and with an injected current $I=980$ mA, corresponding to a steady state electrical power $P=3.2$ W dissipated in the device. The heat sink temperature was kept at $T_H=140$ K. The spectra were measured in backscattering from the laser facets, using parallel polarization to select the contribution of the interface phonon modes. The (*) symbols mark plasma lines of the Kr^+ laser.

The microprobe apparatus used for Raman and PL measurements is described in Ref. 19. We use an interference notch filter to suppress the Rayleigh scattering, and simultaneously record both S and AS spectra. Raman selection rules in backscattering from the edge (110) of the sample allow the observation of IF modes in parallel polarization, i.e., with both incident and scattered photon polarization along the $(1\bar{1}0)$ crystal direction, and the observation of TO phonons in crossed polarization.[20] Both substrate-side and epilayer-side mounted QC lasers were studied. Figure 2 shows two typical S and AS Raman spectra taken from the active region in parallel polarization with the no current flow and with an injected current $I=980$ mA below laser threshold. This corresponds to a steady state electrical power $P=3.2$ W dissipated in the device. The two bands at 226 and 250 cm^{-1} are related to $IF^{I,II}_{InAs}$ and IF_{GaAs} phonon modes, respectively.

The phonon occupation number N can be determined from the ratio ρ between the intensities of S and AS Raman bands[21]

$$N=\left[\rho\frac{\sigma_S(\omega_L)}{\sigma_{AS}(\omega_L)}\left(\frac{\omega_L+\omega_0}{\omega_L-\omega_0}\right)^4-1\right]^{-1}, \quad (1)$$

where $\sigma_{AS}(\omega_L)$ and $\sigma_S(\omega_L)$ are the AS and S Raman cross sections at the laser frequency ω_L. These cross sections have a strong ω_L dependence close to fundamental electronic resonances.[22] In our steady state experiments, Raman signals were detected using $\hbar\omega_L=2.603$ eV, which is more than 1.4 eV far from the strong resonance with the E_0 and $E_0+\Delta_0$ fundamental energy gaps. The notion that no significant resonance effects exists in our devices under the chosen excitation condition and that we can safely use the relation (1) to extract the phonon occupation number N is confirmed by the following arguments. The intensity ratio between two-phonon and one-phonon Raman bands in our spectra is about 4%, which is typical under off-resonance conditions. Moreover, the relation between N_0 and ρ, measured with the device off, can be fitted by the expression (1) using a constant value $\sigma_S(\omega_L)/\sigma_{AS}(\omega_L)=1.040\pm0.015$, in the temperature range 70–350 K.

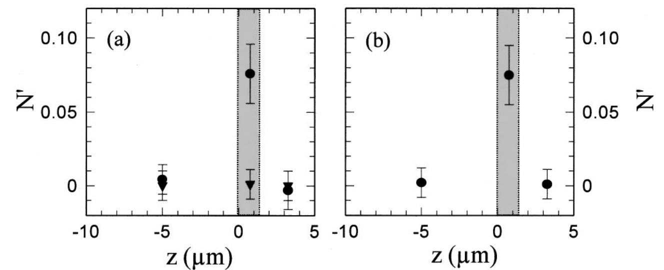

FIG. 3. Excess phonon population N' measured at $T_H=100$ K for the TO mode of InP ($z=5$ μm), the IF_{GaAs} of the active region ($z=0.7$ μm), and the InAs-like TO mode of the AlInAs cladding layer ($z=3.2$ μm): (a) substrate-side mounted QC device with an injected current of $I=900$ mA (●) and $I=2$ mA (▼); (b) epilayer-side mounted QC device with an injected current of $I=850$ mA. The z values refer to different positions along the facet center axis. The origin of the axis corresponds to the interface between the waveguide core and the InP substrate. Positive values indicate the direction toward the AlInAs cladding layers. The lightly shaded regions indicate the waveguide core.

Downloaded 22 May 2008 to 128.103.60.225. Redistribution subject to AIP license or copyright; see http://apl.aip.org/apl/copyright.jsp

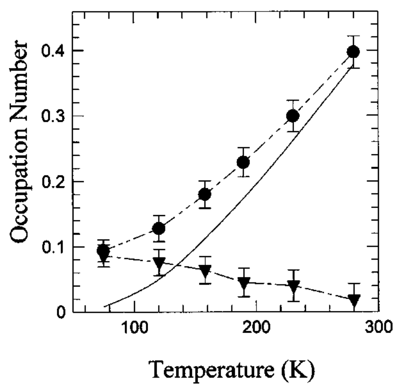

FIG. 4. IF_{GaAs} phonon occupation number N determined by Raman Stokes and anti-Stokes measurements for the substrate-side mounted QC device driven by a cw electrical power of 3.2 W, as a function of the active region lattice temperature (●). The solid curve is a plot of the equilibrium IF_{GaAs} phonon population N_0 calculated from Bose–Einstein statistics in the case of thermal equilibrium with the lattice. $N' = N - N_0$ (▼) is the excess phonon population. The dashed curves are guides for the eye.

The assessment of a nonequilibrium phonon population requires a comparison of the N values extracted from Raman scattering with the thermal equilibrium values N_0. The latter information can be obtained using the microprobe PL technique recently exploited by us for the temperature mapping of QC lasers.[19,23] The local lattice temperatures of operating devices were obtained from the peak positions of PL signals emitted by the different layers composing the QC structure along the facet center axis of the two devices.

Figures 3(a) and 3(b) show that in both QC devices a dissipated electrical power of 3.2 W leads to $N' \sim 0.075$ for the IF_{GaAs} modes of the active region. No IF_{GaAs} hot-phonon populations are observed with an injected current $I = 2$ mA, corresponding to a dissipated power <10 mW. In contrast, the TO modes in the InP, and AlInAs cladding are always in thermal equilibrium with the lattice.

The N and N_0 values for IF_{GaAs} phonons are plotted in Fig. 4 as a function of the active region temperature. The excess phonon population N' decreases monotonically with temperature. The ratio N'/N, which is ~ 1 at low temperature, becomes practically negligible at room temperature. The latter findings are explained considering the enhancement of the background thermal population N_0 and the lowering of the phonon decay time with increasing temperature,[1] and confirm the predictions of recent theoretical calculations.[14,15]

Using the N' values we can estimate the IF_{GaAs} phonon lifetime τ_p following the approach of Ref. 5. In the case of a single interacting phonon, the relation $G_p = (eV/\hbar\omega_s)G_e$ between the electron injection rate G_e and the phonon generation rate G_p per unit volume holds. Here V is the applied voltage and $eV/\hbar\omega_s$ is the number of emitted phonons per electron. In steady state, the phonon generation rate equals the phonon decay rate. Assuming that the optical phonons decay before they equilibrate within the optical branch, and Fröhlich-type interaction, one readily obtains $\tau_p = (2k_p^2/\pi^2) \times (N'/G_p)(k_{max} - k_{min})$, where k_p is the phonon wave vector and k_{min}, k_{max} are the electron wave vector limits. Considering that the scattering rate of IF_{GaAs} phonons is $\sim 25\%$ of the total phonon scattering rates in our system,[17] we estimate a value $\tau_p = 5$ ps at $T = 75$ K and $\tau_p = 2$ ps at $T = 280$ K, comparable with typical values measured for polar optical phonons in III–V semiconductor heterostructures.[1,2]

In summary, we have reported the observation of a steady-state nonequilibrium optical phonon population generated by electron transport in quantum cascade lasers. Our analysis allows us to obtain an estimate of the interface phonon lifetimes, which dominates the electron–phonon interaction in short-period quantum heterostructures. Inclusion of the phonon ensemble in the band structure engineering will give a more realistic description and control not only on the electronic processes and lifetimes, but also on the phonon processes as well. Particularly, the hot-optical phonon population has to be taken into account to design active regions with transition energies close to or below the optical phonons ones, with the aim of achieving QC lasers emitting in the THz range.

This work was partly supported by INFM, Project No. PRA98 "SUPERLAS" and MURST, cluster 26 "Materiali Innovativi," Project No. P5WP2. The work performed at Bell Laboratories was partly supported by DARPA/US ARO under Contract No. DAAD19-00-C-0096.

[1] J. Shah, *Ultrafast Spectroscopy of Semiconductors and Semiconductor Nanostructures* (Springer, Berlin, 1998).
[2] J. A. Kash, Proc. SPIE **942**, 138 (1988).
[3] W. Pötz and P. Kocevar, Phys. Rev. B **28**, 7040 (1983).
[4] P. Lugli and S. M. Goodnick, Phys. Rev. Lett. **59**, 716 (1987).
[5] J. Shah, R. C. C. Leite, and J. F. Scott, Solid State Commun. **8**, 1089 (1970).
[6] D. Y. Oberli, G. Böhm, and G. Weimann, Phys. Rev. B **47**, 7630 (1993).
[7] S. H. Kwok, M. Ramsteiner, D. Bertram, M. Asche, H. T. Grahn, and K. Ploog, Phys. Rev. B **53**, R7634 (1996).
[8] S. M. Komirenko, K. W. Kim, V. A. Kochelap, I. Fedorov, and M. A. Stroscio, Appl. Phys. Lett. **77**, 4178 (2000).
[9] S. M. Komirenko, K. W. Kim, V. A. Kochelap, I. Fedorov, and M. A. Stroscio, Phys. Rev. B **63**, 165308 (2000).
[10] E. M. Conwell, *High Field Transport in Semiconductors*, Solid State Physics, Vol. 9, (Academic, 1967).
[11] V. Narayanamurti, Science **213**, 717 (1981).
[12] C. Gmachl, F. Capasso, D. L. Sivco, Rep. Prog. Phys. **64**, 1533 (2001).
[13] C. Gmachl, F. Capasso, A. Tredicucci, D. L. Sivco, R. Köhler, A. L. Hutchinson, and A. Y. Cho, IEEE J. Sel. Top. Quantum Electron. **5**, 808 (1999).
[14] G. Paulavitius, V. Mitin, and M. A. Stroscio, J. Appl. Phys. **84**, 3459 (1998).
[15] S. Slivken, V. I. Litvinov, M. Razeghi, and J. R. Meyer, J. Appl. Phys. **85**, 665 (1999).
[16] V. M. Menon, W. D. Goodhue, A. S. Karakashian, and L. R. Ram-Mohan, J. Appl. Phys. **88**, 5262 (2000).
[17] F. Compagnone, A. Di Carlo, and P. Lugli, Appl. Phys. Lett. **78**, 2095 (2001).
[18] M. A. Stroscio, J. Appl. Phys. **80**, 6864 (1996).
[19] V. Spagnolo, M. Troccoli, G. Scamarcio, C. Gmachl, F. Capasso, A. Tredicucci, A. M. Sergent, A. L. Hutchinson, D. L. Sivco, and A. Y. Cho, Appl. Phys. Lett. **78**, 2095 (2001).
[20] G. Scamarcio, M. Haines, G. Abstreiter, E. Molinari, S. Baroni, A. Fischer, and K. Ploog, Phys. Rev. B **47**, 1483 (1993).
[21] The intensity of the Raman bands have been extracted by fitting the spectra using a Gaussian line shape for both $IF_{InAs}^{I,II}$ and IF_{GaAs} phonon modes, after subtraction of the known lineshapes associated with the plasma lines at 215.5 and 272.8 cm^{-1}.
[22] T. Ruf, K. Wald, P. Y. Yu, K. T. Tsen, H. Morkoc, and K. T. Chan, Superlattices Microstruct. **13**, 203 (1993).
[23] V. Spagnolo, M. Troccoli, G. Scamarcio, C. Becker, G. Glastre, and C. Sirtori, Appl. Phys. Lett. **78**, 1177 (2001).

Downloaded 22 May 2008 to 128.103.60.225. Redistribution subject to AIP license or copyright; see http://apl.aip.org/apl/copyright.jsp